Proposal to Jefferson Lab PAC 16

CONSTRAINING THE NUCLEON STRANGENESS RADIUS IN PARITY VIOLATING ELECTRON SCATTERING

R. De Leo, L. Lagamba
INFN/Bari

D.J. Margaziotis
California State University

P. Markowitz
Florida International University

R. Wilson
Harvard University

A.T. Katramatou, G.G. Petratos, D.L. Prout
Kent State University

R. Hicks, R. Miskimen, G. Peterson
University of Massachusetts

J. Calarco, W. Hersman, M. Leuschner
University of New Hampshire

G.D. Cates, B. Humensky, K.S. Kumar (Co-spokesperson), D. Relyea
Princeton University

M. Amarian, E. Cisbani, S. Fullani, F. Garibaldi, M. Iodice, R. Iommi, G.M. Urciuoli
INFN/Rome

E. Burtin, C. Cavata, B. Frois, D. Lhuillier (Co-spokesperson),
F. Marie, D. Neyret, T. Pussieux
DSM/DAPNIA/SPhN CEA Saclay

P.A. Souder, R. Holmes
Syracuse University

L. Auerbach, S. Choi and Z. Meziani
Temple University

J.P. Chen, E. Chudakov, K. De Jager, J. Gomez, M. Kuss, J. LeRose,
M. Liang, R. Michaels, J. Mitchell, A. Saha, B. Wojtsekhowski
Thomas Jefferson National Accelerator Facility

D. Armstrong, T. Averett, J.M. Finn, J. Roche
College of William and Mary in Virginia

(This is a Hall A Collaboration Proposal)

ABSTRACT

We propose to measure the parity violating asymmetry in the elastic scattering of 3.2 GeV electrons from a liquid Hydrogen target in Hall A at a scattering angle of $\theta_{\rm lab} = 6^\circ$, corresponding to an average Q^2 of 0.11 $(\mathrm{GeV/c})^2$. The small scattering angle will be achieved with a combination of the HRS high resolution spectrometers and septum magnets that are planned to be installed in Hall A. The physics asymmetry is estimated to be about 1.7 parts per million. With 100μA electron beam and a polarization of 75%, a statistical error of 4.6% and a projected systematic error of 2.9% can be achieved in 700 hours. The recent physics run of the HAPPEX experiment has demonstrated that systematic errors can be controlled at the required level with a high polarization photocathode.

This measurement would access the linear combination $\rho_s + \mu_p \mu_s$ to an accuracy of ± 0.31 and would provide a direct sensitive constraint on the nucleon strangeness radius. The experiment would thus probe the importance of strangeness to the charge distribution inside nucleons and could potentially make a clean, nonzero measurement of a nucleon strangeness matrix element.

I INTRODUCTION

Several lepton and hadron scattering experiments have recently focused on the issue of the strange structure of the nucleon. Establishing a nontrivial role for the nucleon sea would provide spectacular evidence for new nonperturbative strong dynamics. While there are intriguing suggestions for nonzero strange matrix elements, there is no consensus in the theoretical interpretation of the results.

Measurements of parity violating asymmetries in elastic electron scattering are a natural way to access vector strange matrix elements [1,2]. Recently, the SAMPLE [3] and the HAPPEX [4] experiments have carried out measurements of such asymmetries off protons at $Q^2 \sim 0.1$ (backward angle) and 0.5 $(\mathrm{GeV/c})^2$ (forward angle) respectively. In parallel, theoretical models have tackled quantitatively the leading nonzero moments of the strange quark form factors: the strange magnetic moment μ_s and the strangeness radius ρ_s [5]. The results of the abovementioned pioneering experiments have ruled out a large value of μ_s and suggest that if ρ_s is large then the strange form factors must fall rapidly with Q^2. However, there is as yet little theoretical guidance on the Q^2 dependence of the strange form factors.

We propose a new measurement that focuses on the leading moments with little sensitivity to the Q^2 dependence of the form factors. In this proposal, we would measure the parity violating asymmetry in the elastic scattering of 3.2 GeV electrons from protons at $\theta_{\mathrm{lab}} = 6^\circ$ ($Q^2 = 0.11$ $(\mathrm{GeV/c})^2$) in Hall A. A relative accuracy of $\pm 4.6\%$(stat) $\pm 2.5\%$(syst) $\pm 1.4\%$(theo) can be achieved in 700 hours at a beam current of 100 μA and a beam polarization of 75%. From this measurement, we would obtain the linear combination $\rho_s + \mu_p \mu_s$ with an accuracy of ± 0.31. When combined with the anticipated uncertainty of the SAMPLE experiment, the Dirac strangeness radius $\langle r_s^2 \rangle$ would be constrained to $\pm 0.04 fm^2$.

The experiment is a natural sequel to the HAPPEX measurement, which established the feasibility of high accuracy, high luminosity parity violation experiments in Hall A at Jefferson Lab. The most recent run of the HAPPEX experiment has further demonstrated that the potentially larger systematic problems associated with the high polarization strained photocathode can be controlled at the required level.

II PHYSICS MOTIVATION

The Valence Quark Model has provided valuable insights into the structure of baryons. On the other hand, the dynamical origin of the nucleon sea remains elusive. Indeed, one of the central issues in nucleon strong dynamics today is the justification of the success of the Quark Model: why is the $q\bar{q}$ sea, which originates from nonperturbative effects, so highly inert? It is thus interesting

to probe asymmetries and moments of sea quark distributions experimentally. Indeed, different theoretical approaches produce widely differing predictions for various sea quark distributions.

Strange quarks are a direct, pure probe of the nucleon sea and thus a particularly fertile testing ground for various QCD models. Since $m_s \sim \Lambda_{\rm QCD}$, it is quite plausible that strange quarks play a nontrivial role in determining fundamental bulk nucleon properties. On the other hand, the empirically successful OZI rule suggests that strange quark effects are highly suppressed at low energy. The issue must be settled by experiment. However, the goal of making a compelling measurement of a strange matrix element has proved to be challenging.

Experimental measurements to date come from the area of $\pi - N$ and spin dependent deep inelastic lepton scattering experiments. Spin structure function measurements indicate that only ~30-40% of the proton spin is carried by quarks. When this data is combined with measurements of hyperon decay rates, the resulting analysis suggests that ~10% of the proton spin is carried by strange quarks. However, this effect may be explained by flavor SU(3) breaking and is an area of active theoretical and experimental debate. An additional indication comes from the pion σ term from an analysis of low energy $\pi - N$ scattering, which suggests that the strange quark scalar matrix element contributes significantly to the proton mass.

II.1 Parity Violating Electron Scattering

The results described above motivate the search for other strange matrix elements. A clean experimental technique [6] for isolating vector strange matrix elements is by measuring parity-violation amplitudes in the elastic scattering of polarized electrons from nucleons and nuclei [1,2]. One measures an asymmetry defined by

$$A^{PV} = \frac{\sigma_R - \sigma_L}{\sigma_R + \sigma_L} \tag{1}$$

where σ_R (σ_L) is the scattering cross section using incident right (left) handed electrons.

The theoretical asymmetry is given in the Standard Model by [5]

$$A^{PV} = \left[\frac{-G_F Q^2}{\pi\alpha\sqrt{2}}\right] \times \frac{\varepsilon G_E^{p\gamma} G_E^{pZ} + \tau G_M^{p\gamma} G_M^{pZ} - \frac{1}{2}(1 - 4\sin^2\theta_W)\varepsilon' G_M^{p\gamma} G_A^{pZ}}{\varepsilon (G_E^{p\gamma})^2 + \tau (G_M^{p\gamma})^2} \tag{2}$$

where G_F is the Fermi coupling constant and $G_E^{p\gamma}(G_M^{p\gamma})$ is the electric(magnetic) Sachs form factor for photon exchange, $G_{E,M}^{pZ}$ is the corresponding quantity for Z^0 exchange and θ_W is the electroweak mixing angle. All form factors are functions of Q^2 and ε, τ, and ε' are kinematic quantities.

To interpret the experiment, $G_{E,M}^{p,Z}$ can be expressed in terms of proton, neutron, and strange form factors if the up(down) quarks in the proton have the same properties as the down(up) quarks in the neutron (assumption of isospin symmetry). Then

$$G_{E,M}^{p,Z} = \frac{1}{4}(G_{E,M}^{p\gamma} - G_{E,M}^{n\gamma}) - \sin^2\theta_W\, G_{E,M}^{p\gamma} - \frac{1}{4}G_{E,M}^{s} \tag{3}$$

and, if the electromagnetic form factors are sufficiently well known from experiment, the only unknown quantities involve strange form factors.

II.2 Theoretical Predictions

Given the impact of potentially large strange quark effects in the nucleon, significant theoretical effort has been applied to obtaining a quantitative understanding of the strange quark form factors. This is challenging and effort has been focused on the leading nonzero moments of the strange quark form factors:

$$\mu_s \equiv G_M^s(0); \quad \rho_s \equiv \left.\frac{dG_E^s}{d\tau}\right|_{\tau=0}. \tag{4}$$

It is often more convenient to talk about a strangeness Dirac rms radius, in analogy to the charge radius, which is related to the above quantities as follows:

$$\langle r_s^2\rangle \equiv -6\frac{dF_1^{s2}}{dQ^2}; \quad \rho_s = -\frac{2}{3}M_p^2\langle r_s^2\rangle - \mu_s. \tag{5}$$

Here, F_1^s is the Dirac strange form factor and M_p is the nucleon mass.

Lattice QCD, hadronic models and effective hadronic theory are three broad approaches that have been used to estimate the abovementioned quantities [7]. Theoretical predictions vary widely and are not consistent in the predicted sign for ρ_s. Further, at this stage there is little insight into the Q^2 dependence of the form factors. We present a brief discussion on some aspects of the literature below as an introduction. Some of the results on the leading moments are tabulated in Table 1.

One approach is to use dispersion theory fits to the nucleon isoscalar form factors [9], updated to account for new data and constraints from peturbative QCD at large Q^2 [10]. Such an approach predicts a sizeable strange radius. On the other hand, it has been pointed out that the inclusion of $\pi\rho$ correlated exchange is significant and might reduce the predicted size of the strange vector form factors [11]. The authors of Ref. [12] added the $K\bar{K}$ continuum contribution in addition to the usual vector meson poles. They found that the magnitude and sign of μ_s is rather robust but find that predictions for ρ_s vary over a wide range.

Source	$r_s(fm^2)$	ρ_s	μ_s	$\rho_s + \mu_p\mu_s$	Reference
Poles	0.16	-2.10	-0.31	-2.97	[9]
Poles (update)	0.21	-2.93	-0.24	-3.60	[10]
Poles + $K\bar{K}$	-0.15 - +0.42	-6.0 - +2.65	-0.51 - -0.26	-7.10 - -1.23	[12]
NJL model	-0.2	3.06	-0.05	2.92	[13]
SU(3) Skyrme	-0.19	3.19	-0.33	2.27	[14]
SU(3) Skyrme broken sym.	-0.10	1.64	-0.13	1.27	[15]
Lattice	-0.16 - -0.06	1.26 - 2.77	-0.56 - -0.16	0.25 - 1.76	[16]
Quark Model	-0.04	0.57	0.035	0.67	[17]

TABLE 1. Various predictions of the strangeness radius and magnetic moment.

In addition to the dispersion approach, there exists a quark model calculation in which a sum over a tower of OZI-allowed states is performed [17]. The authors find that both the leading moments are small. Recently, lattice QCD techniques have also begun to yield predictions for the leading moments of the strange form factors [16].

In summary, predictions for μ_s are either very small or fall within the range -0.2 to -0.4 μ_N. Predictions for ρ_s on the other hand vary over a large range and are typically considered more speculative in most approaches. The HAPPEX experiment that is currently running in Hall A is the first experiment to have significant sensitivity to the strange electric form factor. The projected sensitivity from the '99 run on ρ_s depends on the assumed Q^2 dependence of the strange form factors, but a conservative estimate is that the sensitivity of the measurement is roughly the size of the neutron charge radius. Our measurement would provide a constraint that is three times smaller than the size of the neutron charge radius. Such sensitivity would access the range of values favored by theoretical predictions and would address whether strangeness is an important degree of freedom in the charge distribution inside nucleons.

II.3 Experimental Strategy

From Table 1, it is clear that a measurement of $\langle r_s^2 \rangle$ to better than ± 0.05 would be an important step in addressing the issue of strangeness in nucleons. In order to achieve this level of accuracy, we wish to go to sufficiently low $Q^2 (\sim 0.1$ (GeV/c)$^2)$ so that information on the leading moments ρ_s and μ_s can be obtained with little dependence on the Q^2 behavior of the form factors.

Our first priority in optimizing the experimental design is to obtain a sensitive measurement of ρ_s, on which no clean experimental constraints are available to date. The best available constraint can be derived from the HAPPEX measurement at $Q^2 = 0.48$ (GeV/c)^2, though additional assumptions on the Q^2 dependence for the strange electric as well as magnetic form factors are required. The projected errors (when the '99 data is analysed) range from ± 0.05

to $\pm 0.12 fm^2$, depending on assumptions. The two logical target choices for new measurements at low Q^2 are ^{1}H and ^{4}He.

Hydrogen has the advantage that one is directly probing the nucleon and one can employ a dense target. Further, the fractional error on the asymmetry that leads to useful constraints on strangeness tends to be at the 10% level. One disadvantage is that one is measuring the linear combination $\rho_s + \mu_p \mu_s$. Additionally, as Q^2 is lowered, the nuclear structure independent piece of the asymmetry ($1 - 4\sin^2\theta_W$ term in Eq. 6) begins to dominate the weak neutral coupling so that it becomes increasingly difficult to obtain precise information on the form factors.

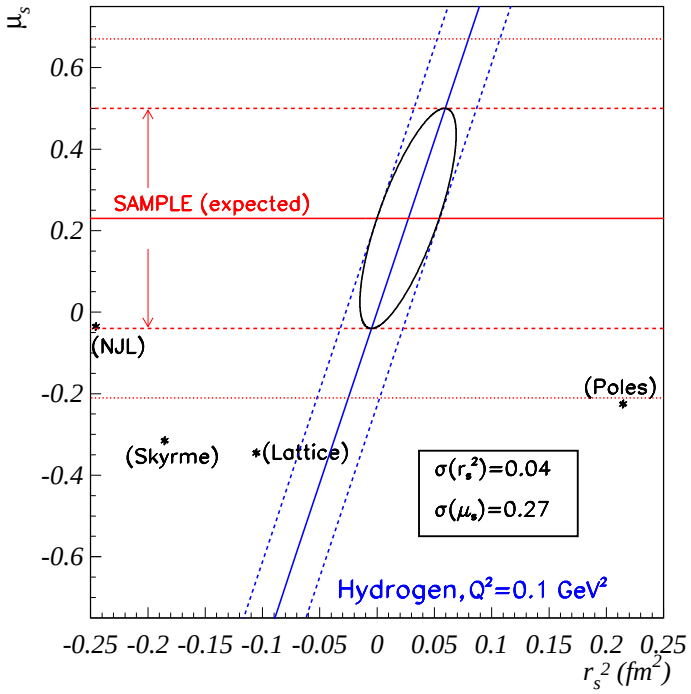

FIGURE 1. The sensitivity of the proposed ^{1}H measurement is shown. Also shown are the published and projected errors from the SAMPLE experiment, centered at the published value. Stars correspond to various theoretical predictions listed in Table 1.

Helium has the advantage that one is directly measuring ρ_s. Moreover, the theoretical ambiguities in considering the nucleus as a spinless, isoscalar coherent state of four nucleons are estimated to be small. The disadvantages are that it is difficult to get a target as dense as that for hydrogen and further, one needs to measure the asymmetry at the 5% level in order to obtain useful constraints on strangeness.

We have investigated the feasibility of both measurements and find that they lead to similar constraints on the strange radius for the same beam current. This proposal focuses on ^{1}H for two technical reasons. Firstly, the target

system for hydrogen already exists and has been demonstrated to work at the highest luminosities that we propose to use for this experiment. Secondly, the absolute normalization for ^{1}H is less stringent than that required for the ^{4}He measurement. Figure 1 shows the achievable errors on $\langle r_s^2 \rangle - \mu_s$ from the ^{1}H measurement. Also shown are the current and anticipated error bars of the SAMPLE experiment.

III CHOICE OF KINEMATICS

The choice of our running conditions is driven by our sensitivity to the linear combination $(\rho_s + \mu_p \mu_s)$. Using the definition of Eq.(4) and expanding the expression of the parity violating asymmetry (2) to first order in Q^2 yields

$$A^{PV} = -\frac{G_F Q_2}{4\pi\alpha\sqrt{2}} \left[(1 - 4\sin^2\theta_W) + \tau(\mu_n - \rho_s - \mu_p(\mu_n + \mu_s)) \right] + \mathcal{O}(\tau^2) \quad (6)$$

where we have used the small angle approximations $\epsilon' \simeq 0$, $\epsilon \simeq 1$, and $\tau \ll 1$. The absolute statistical error on $\rho_s + \mu_p \mu_s$ is then

$$\delta(\rho_s + \mu_p \mu_s) = \left(\frac{1 - 4\sin^2\theta_W}{\tau} + \mu_n(1 - \mu_p) \right) \times \frac{\delta A^{PV}}{A^{PV}} + \mathcal{O}(\tau^2) \quad (7)$$

Figure (2) shows the corresponding figure of merit (FOM) as a function of the two free parameters of the elastic kinematics, the scattering angle and the beam energy. We can see that at very low Q^2 (small θ and low E_{beam}), the

E_{beam} (GeV)	θ (deg)	Q^2 (GeV^2)	$d\Omega$ (msr)	$\delta A^{PV}/A^{PV}$ (%)	$\delta(\rho_s + \mu_p \mu_s)$
3.2	6.00	0.110	2×3.60	4.3	0.25
2.4	7.64	0.100	2×3.60	5.9	0.35
1.6	12.50	0.117	2×5.50	6.7	0.38

TABLE 2. Projected statistical error bars after 700h beam time for three kinematics at $Q^2 \simeq 0.1\,GeV^2$. Detection below 12.5° requires a septum magnet which reduces the acceptance of the spectrometer. A cut in the radiative tail is applied at 1% of the elastic energy. Results are obtained from average values in the plane of the collimator.

sensitivity to strangeness in the nucleon falls off. Simulations including finite acceptance and extended target effects, as well as radiative corrections show that the best compromise is to relax the constraint on the beam energy and stay at small scattering angle to take advantage of the high counting rates.

Assuming a 100μA beam current, 75% beam polarization and the target properties given in Table 5 we then obtain a luminosity of $\mathcal{L} = 3.96 \times$

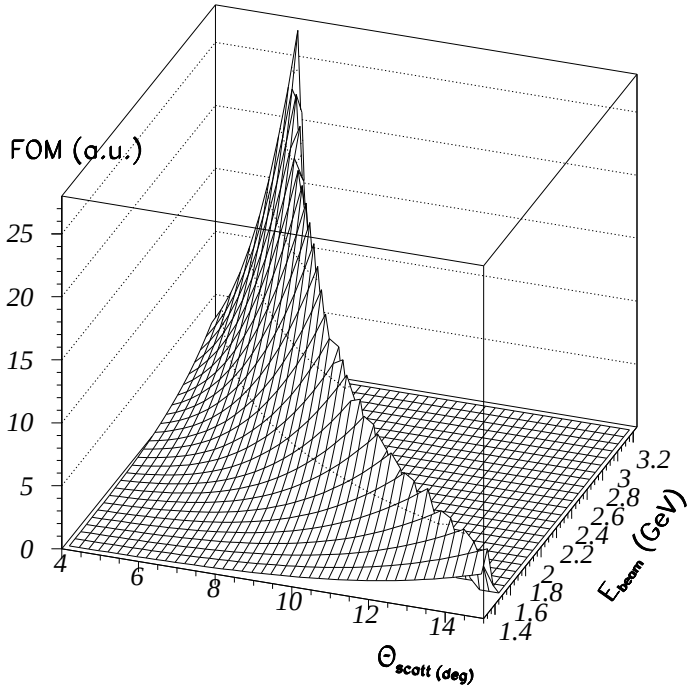

FIGURE 2. Figure Of Merit for the measurement of strange form factors in elastic e-P scattering. Only the kinematical domain $Q^2 < 0.25\,GeV^2$ is represented. The plotted quantity is the square of $\delta(\rho_s + \mu_p\mu_s)^{-1}$ (Eq.7). The solid angle is assumed constant over all the kinematic range, the elastic cross section is calculated using a dipole form factor and the contribution from strange quarks is set to zero in the parity violating asymmetry.

$10^{38}\,cm^{-2}s^{-1}$. Table 2 shows the projected statistical error bars after 700h with these running conditions for three kinematic points at $Q^2 \simeq 0.11$ GeV^2. The current minimum central angle of the Hall A HRS is 12.5°. To go to smaller scattering angles, our experiment will use septum magnets, inserted between the scattering chamber and the entrance of the HRS. This apparatus is being designed by the Hall A Hypernuclear Collaboration [18] and will be mounted next year. It will allow the detection of scattered electrons as forward as 6°. The HRS pair can detect electrons with a maximum momentum of 3.1 GeV. We therefore choose to run the experiment at this minimum angle and a beam energy of 3.2 GeV.

Rates and kinematics corresponding to $E_{beam} = 3.2$ GeV and $\theta = 6°$ are listed in Table 3. Central and average values are comparable because of the cancellation of two main effects. The finite acceptance opens the phase space to larger scattering angles, which decreases the cross section. On the other hand, emission of real photons by the electrons lowers the effective Q^2 and thus increases the mean cross section. Figure 3 plots the expected statistical error bars for the asymmetry and the accessed linear combination of the strange

	θ (deg)	Q^2 (GeV^2)	$d\Omega$ (msr)	$d\sigma/d\Omega$ ($\mu b.sr^{-1}$)	A^{PV} (ppm)	Rate (Mhz)
Central Value	6.00	0.110	2×3.57	44.83	-1.67	127.8
Average Value	5.93	0.109	2×3.57	44.45	-1.63	126.8

TABLE 3. Central values correspond to the kinematics of a scattered electron following the reference trajectory of the spectrometer. Average values take into account the effects of finite acceptance, extended target, radiative losses and tracking through the spectrometers. The cut in the radiative tail is taken to be 1% of the energy of the elastic peak ($\Delta E \simeq 30MeV$, 10% losses). The quoted counting rates include the sum over the two Hall A spectrometers. Values of A^{PV} are for 100% beam polarization.

form factors as a function of the beam time:

$$\frac{\delta A^{PV}}{A^{PV}} = \frac{1}{P_e A^{PV}} \times \frac{1}{\sqrt{\mathcal{L}\frac{d\sigma}{d\Omega}d\Omega}} \times \frac{1}{\sqrt{T}}$$

$$\delta(\rho_s + \mu_p \mu_s) = \left[\frac{1 - 4\sin^2\theta_W}{\tau} + \mu_n(1 - \mu_p)\right] \times \left[\frac{\delta A^{PV}}{A^{PV}}\right]$$

A statistical accuracy of 4.6% is achievable in the asymmetry in 700 hours. The corresponding uncertainty in the linear combination of ρ_s and μ_s is $\delta(\rho_s + \mu_p\mu_s) = \pm 0.25$.

IV APPARATUS

The experimental design is driven by the fact that one is measuring a small parity violating asymmetry of the order of 1 part per million (ppm). To measure such an asymmetry with little contamination from spurious effects, one needs to rapidly flip (in time) between the two possible electron helicity states while keeping all other experimental parameters virtually unchanged. One then averages the fractional difference in the cross-section over many pairs of beam "windows" of opposite helicity.

Our measurement technique will follow the methods employed for the published HAPPEX measurement which takes advantage of the high resolution spectrometers in Hall A. We note the key features:

- We integrate the scattered flux over each helicity window. The current set up has already been demonstrated to work at 50 MHz and can be realistically extrapolated to 200 MHz.
- The scattered flux from each spectrometer is digitized using custom built ADCs.

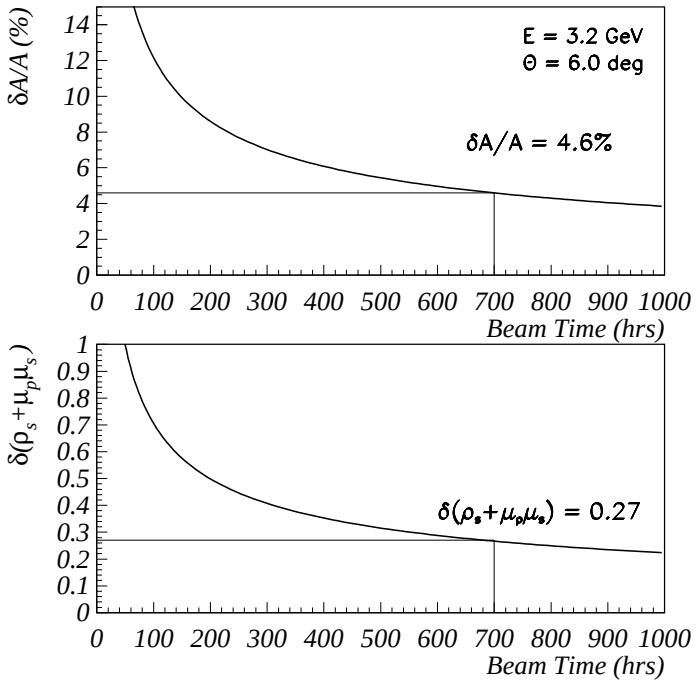

FIGURE 3. Projected statistical errors on the asymmetry and the first momenta of strange form factors. Quoted values are for 700h beam time.

- Separate low rate runs in counting mode would demonstrate that the backgrounds are negligible.
- The electron beam would be dithered systematically in position, angle and energy in order to measure the sensitivity to false asymmetries from helicity correlated fluctuations in the beam parameters.
- The helicity correlated intensity asymmetry will be kept below 10^{-7} using an active feedback loop.

In the following, we briefly describe the main components of the experiment.

IV.1 Polarized Electron Source

Polarized electrons are produced by photoemission from a strained GaAs photocathode illuminated by an IR pulsed laser at 499 MHz (1/3 of the frequency of the accelerating cavities). The laser light is polarized by a Pockels cell which allows rapid helicity reversals up to several tens of Hz. The most important requirement for our experiment is the stringent control of helicity correlations in the laser light impinging on the photocathode. Indeed most of

Energy	3.2 GeV
Intensity	100 μA CW
Polarization	75%
Frequency of helicity reversal	30 Hz
Raster size	2mm$\times$2mm

TABLE 4. Beam properties.

the helicity correlations in the electron beam can be traced back to helicity correlations in the physical characteristics of the laser light.

The ongoing HAPPEX run with a high polarization cathode has demonstrated that systematic corrections can be maintained at a level that is sufficient for the purposes of this proposal. This will be discussed briefly in Section *V*.1.2. Required beam characteristics are listed in Table 4.

IV.2 Target

This experiment will use the liquid hydrogen cryo-target operating in Hall A. Main specifications are listed in Table 5. The target has already been operated at the required 100 μA for various physics experiments. For measuring high rates and small asymmetries our greatest concern is the density fluctuation. The rapid helicity reversal of the beam eliminates variations over long time periods. However, small random fluctuations due to boiling that might average out during a cross section measurement might add noise to the

Refrigeration capacity	700 W
Operating temperature	20 K
Operating Pressure	26 psia
Density	0.0708
Length	15 cm
Thickness	1.1 g/cm^2
Beam load at 100 μA	400 W

TABLE 5. Liquid Hydrogen target specifications.

data that would appear as statistical fluctuations significantly larger than that predicted by counting statistics. A limit of 2×10^{-4} was placed during the HAPPEX commissioning run, which is barely sufficient for this proposal. We plan to take data at 120 Hz (while still flipping the beam helicity at 30 Hz), in order to alleviate this effect.

IV.3 Spectrometers

Both Hall A High Resolution Spectrometers will operate at symmetric angles to double the statistics. They will be positioned to their minimal central angle (12.5°) corresponding to 6° at the entrance of the septum magnet (Fig.5). The HRS pair is ideally suited for the high rate integration technique, since the

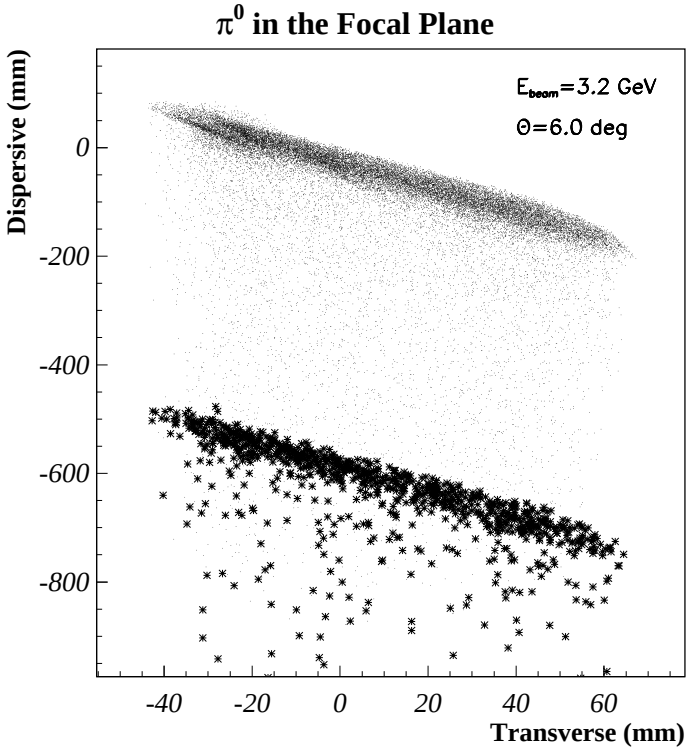

FIGURE 4. Distribution of scattered electrons in the focal plane for $E_{beam} = 3.2GeV$ and $\theta = 6°$. Black dots and stars correspond to elastic and π^0 production events respectively. A 60 cm gap separates the elastic from the inelastic scattered electrons. This simulation uses flat cross section so the relative amount of events is not correct.

elastically scattered electrons must be focused on to a region that is otherwise free of background into total absorption counters. For this experiment, as in the case of the HAPPEX measurement, the elastic electrons are focused on to the focal plane along a thin stripe. A total absorption calorimeter with a single phototube will be placed on the focal plane to intercept this stripe. The output of this device will be integrated over the duration of each beam helicity window.

Figure 4 shows the distribution of the elastically scattered electrons as well as events close to the π^0 threshold. The simulation uses the ray tracing program "snake" which includes high order matrix elements. We obtain a gap of 60 cm between the elastic and inelastic events which is very comfortable.

IV.4 Septum magnets

The septum magnets, originally designed for hypernuclear physics ([18,19]), allow experiments using scattering angles smaller than the current minimum of 12.5°. With a 6.5 horizontal bending angle, this magnets extend the angular range down to 6°. A layout is shown in Figure 5. The physical

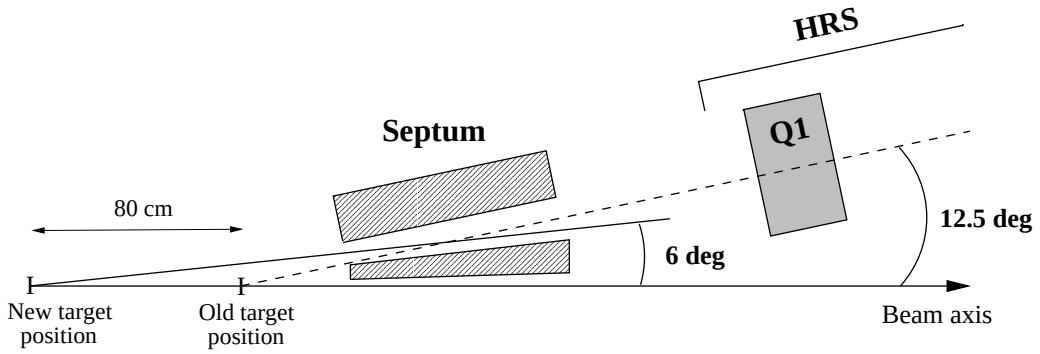

FIGURE 5. Layout of the septum insertion. To stay on the optical axis of the two spectrometers, the target will be moved upstream 80 cm.

aperture corresponds to a solid angle of 4.7 msr but additional cuts in the acceptance must be applied. A Monte Carlo including the tracking through the magnetic optics and extended target effect gives a solid angle of 3.95 msr. This result is quite sensitive to the quadrupoles tuning which could be further optimized. We will participate in the commissioning of these magnets and use data from early experiments to examine issues of acceptance and background.

IV.5 Focal Plane Detector

The very high counting rates at forward angle (Fig.6) excludes the acquisition of individual events. The signal of the elastically scattered electrons will be integrated over each helicity window. The same technique already validated by HAPPEX and based on a radiator-fiber sandwich will be used. Above the 1 MHz/cm^2 counting rate level, a new concern might be radiation hardness. Extended studies going on for LHC experiments [20] show that quartz fibers should be a good substitute for the lucite currently used as the light guide. The dimensions of the detector have to fit with the image of the elastic peak in the focal plane. Although Figure 4 tends to show that a large part of the radiative tail could be integrated in a wide detector, one has to take care of background coming from rescattering in the spectrometer (see background section below).

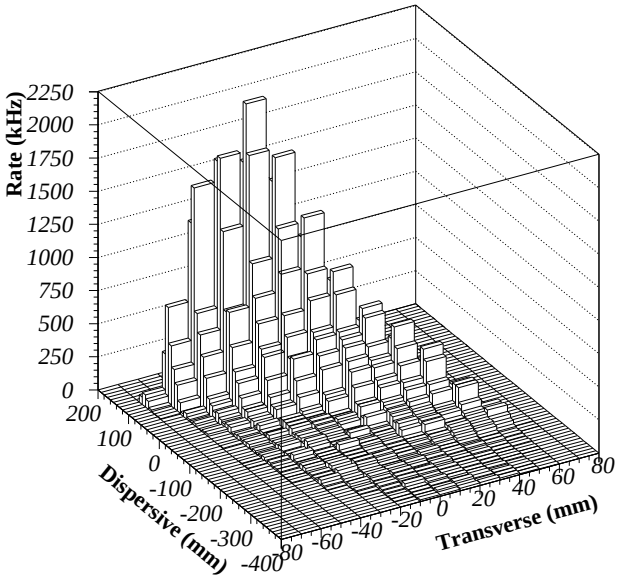

FIGURE 6. Counting rates per cm^2 in the focal plane for a 3.2 GeV beam and a 6° scattering angle.

V SYSTEMATICS

V.1 Asymmetries

One of the challenging aspects of the experiment is that the statistical error in the raw asymmetry will be 5×10^{-8}. We plan to control false asymmetries due to spurious helicity correlations in the beam to be less than 5×10^{-8}, so that systematic errors associated with corrections to the raw asymmetry are negligible. To achieve the statistics in a reasonable length of time, the experiment will detect electrons at approximately 120 MHz. The challenges associated with the abovementioned numbers is the focus of this section.

V.1.1 Random Fluctuations

We plan to flip the helicity of the beam at 30 Hz, using the same scheme as that used by the HAPPEX experiment. The helicity of the beam is picked pseudorandomly at 15 Hz. This determines the helicity of the first pulse in a pair of 30Hz windows. The second pulse in the pair is then the complement of the first. Therefore, "window pair" asymmetries are measured at the rate of 15 Hz. The statistical error for each window pair is about 350 ppm for our kinematics.

In the experimental design, one must ensure that all sources of instrumentation noise contribute less than 100 ppm to the window pair asymmetry.

During the HAPPEX measurement, only one contribution failed to satisfy the abovementioned requirement: the target density fluctuations, which was measured to be about 200 ppm at 100μA. Two ways to alleviate this problem is to take data at 120 Hz and increase the size of the beam spot on target. We believe that either one of these changes would reduce the noise below the required level.

Measurement of the beam flux poses no problems, since the pedestal noise was found to be about 40ppm, as measured by comparing fluctuations from two different beam current monitors in the hall. For the relative flux, the pedestal noise was found to contribute about 100 ppm. Finally, there is the effect of electron beam fluctuations in position. The beam jitter on the target was found in HAPPEX to be about 10μm, which contributes less than 20 ppm to the window pair asymmetry and is thus negligible.

V.1.2 Helicity Correlated Fluctuations

The helicity correlations in the beam are an important challenge in a parity violation experiment. Most of the spurious helicity correlations on target originate from helicity correlations in the laser beam that strikes the photocathode. It is therefore of utmost importance to reduce the helicity correlations in the laser beam to be small or negligible.

In the recent HAPPEX run, we have demonstrated that we can control the helicity correlated intensity asymmetry to better than 5×10^{-7}. This would ensure that the systematic error from the beam flux normalization is negligible (assuming atmost 1% alinearity). We have further learnt to control the average helicity correlated position asymmetry on the target to be less than 20 nm, which limits corrections due to position fluctuations at the level of 2×10^{-7}. We will continue our collaboration with the Jlab polarized source group to reduce these fluctuations even further. This work will involve manipulating the phase retardation of laser light as well as introducing helicity-correlated position differences into the laser beam. For this proposal, modest improvements over the limits achieved for HAPPEX will be sufficient to ensure that the systematic error from corrections due to helicity correlated beam fluctuations are small compared to the statistical error.

The beam monitoring devices and the beam dithering devices used to study the sensitivity of the cross section to helicity correlations in the beam parameters will be identical to that being used currently for the HAPPEX experiment.

V.2 Normalization

V.2.1 Polarimetry

At the present time, the Mott and Moller polarimeters give us two independent measurements of the beam polarization with a relative error of 3%. These performances are already sufficient for our experiment on hydrogen. The main uncertainty in the Moller results comes from the polarization of the target and there is good hope to reduce the overall precision to 2%. A third device, the Compton polarimeter, is now installed on the Hall beam line and is able to measure the polarization simultaneously with data taking, eliminating errors due to time variation in the polarization. At 3.2 GeV and $100\mu A$, a 1% statistical error is reached within 20 minutes. The systematics are still being studied and we hope to use this polarimeter for future experiments with similar accuracy.

V.2.2 Background

All the background intercepted by the focal plane detector will be integrated in our signal as well. A careful estimate of the background is thus necessary. Backgrounds uncorrelated to the beam helicity will induce a dilution factor in the experimental asymmetry. If part of this background is correlated with the helicity reversal, a contribution will also remain in the numerator, leading to a false asymmetry. An empirical study of backgrounds has been performed by R.Michaels for HAPPEX [21] highlighting three main sources of systematic errors:

- *Pollution from quasi-elastic scattering in the end caps*:
  At HAPPEX where the scaterring angle was 12.5°, the fraction of background in the whole focal plane was estimated to be 1.5%. For a scattering angle of 6° the relative contribution of the quasi-elastic peak is enhanced [22] by a factor 2 and the target endcaps appear more internal to the spectrometer acceptance giving rise to another factor two. On the other hand, assuming a width of the focal plane detector equivalent to 30 MeV on both sides of the elastic energy, only 60% of the quasi-elastic events are intercepted.
  Assuming a 25% error in the electroweak asymmetry for the quasielastic scattering we obtain a systematic error of 0.75%.

- *Rescattering of electrons associated with pion production*:
  The momentum resolution of the Hall A spectrometers ensures that no event above the pion production threshold can be seen directly by the focal plane detector. Nevertheless, some electrons with momentum below the acceptance range can hit somewhere the spectrometer frame and be

scattered back into our detector. Following the strategy of the HAPPEX experiment, measurements of counting rates for a set of dipole fields will be carried out. The background should be significantly reduced compared with HAPPEX since the ratio of inelastic to elastic cross sections is reduce by a factor 5.

- *Moller scattering in iron*:
  Iron at the front of the spectrometer dipole acts as a collimator. Some of the electrons can lose some energy by Moller scattering from the polarized electrons in the iron and be detected in the focal plane. The potential asymmetry of this process is orders of magnitude above the parity violating asymmetry but because of the weak fraction of rescattered electrons and the angle between the magnetization and the spin of the incident electron, the effect was found to be much less than 0.1% for HAPPEX. For this experiment the measured asymmetry is almost 10 times smaller so we project a conservative systematic error of 0.5%.

Adding in quadrature the two main contributions we obtain a systematic error of 0.9%.

V.2.3 Determination of the mean Q^2

Since the parity violating asymmetry varies linearly with Q^2, the average value of Q^2 over all the spectrometer acceptance of the HRS has to be known with a good accuracy. We plan to measure this quantity by taking data in counting mode at low current. The main uncertainty comes from the reconstruction of the scattering angle. With a careful survey, the absolute angle of the spectrometers can be known to 0.3 mrd. Error on the angle reconstructed by the drift chambers is $\simeq$ 0.3 mrad on an event by event basis. This error cancels out with sufficient statistics. The final relative systematic error on the asymmetry is 0.6%.

V.3 Theoretical uncertainties

V.3.1 Neutron form factors

Extraction of the strange form factors from the parity violating asymmetry assumes the knowledge of electromagnetic form factors. While the proton form factors have been extensively and accurately measured, substantial uncertainties still remain for the neutron electric form factor. Experimentally, G_E^n is known from electron scattering off light nuclei (deuteron, ^3He). The form factor is deduced from a NN potential and the main uncertainty comes from the differences between different models. In [24], the following parameterization is used

$$G_E^n(Q^2) \;=\; -a\mu\tau G_D(Q^2)(1+b\tau)^{-1} \tag{8}$$

where μ is the neutron magnetic moment and a, b are free parameters. Depending on the NN potential used, the best value of a and b fitted on the experimental data lead to a 33% uncertainty in the G_E^n normalization at $Q^2 = 0.11\,GeV^2$. Nevertheless, the absolute precision is pinned down at low Q^2 by the accurate value of the slope of the form factor near $Q^2 = 0$ (parameter a) measured in thermal neutron-electron scattering [23]. Considering the only fits consistent with this slope we get a $\pm 6\%$ error on G_E^n (the whole set of fits with the parameter a constrained gives $\pm 20\%$). The error in the asymmetry is then identified with the difference in A^{PV} between G_E^n being its maximum and minimum value. We neglect the uncertainty on G_M^n at low Q^2. The final systematic error in the asymmetry is then 1.4% (4.8% with the complete set of fits).

V.3.2 Radiative corrections

Assuming the validity of the standard model at low energy, the main uncertainty comes from running the electroweak couplings in Q^2 from the precise high energy measurements. We use weak radiative corrections calculated at $Q^2 = 0$ compiled in Particle Data Tables [25]. Since these values vary slowly with Q^2, they are considered to be valid for our kinematics. The axial vector contribution has large uncertainty in its weak radiative corrections but fortunately the whole axial term is highly suppressed at forward angle (only 1.5% contribution to the asymmetry). Final systematic error in the asymmetry is estimated to be $\delta A^{PV}/A^{PV} = 1\%$.

V.4 Error Budget

The experimental errors are given in Table 6. The uncertainty on G_E^n is quoted separately since it depends on future experimental results.

VI BEAM TIME REQUEST

We request 700 hours of production running with 100μA of 75% polarized electron beam (assuming 100% efficiency). The septum magnets will be installed prior to our production run for another approved experiment. We will need about 24 hours additional setup and checkout time to align our calorimeter with respect to the elastic peak and measure Q^2 and background at low current. The total time is 724 hours or 30 days. Based on our experience with the HAPPEX experiment, an overall efficiency of 50% of the production running time would easily account for all the physics data, background and Q^2 measurements and beam polarization measurements.

Source	$\delta A^{PV}/A^{PV}$	$\delta(\rho_s + \mu_p\mu_s)$
Statistics	4.6%	0.267
Polarimetry	2.0 %	0.116
Background	0.9 %	0.052
Q^2	0.6 %	0.035
Radiative Corrections	1.0 %	0.058
Subtotal	5.2 %	0.303
G_E^n	1.4 % (4.8%)	0.081 (0.278)
Total	5.4 % (7.1%)	0.314 (0.411)

TABLE 6. Error budget.

VII RELATION TO OTHER EXPERIMENTS

The SAMPLE and HAPPEX experiments are the first parity violation experiments dedicated to the measurement of the strange vector form factors. As first generation experiments, they were optimized to see anomalously large effects. When these experiments are completed, the sensitivity to μ_s will be at the level of 0.25 μ_N and to $\langle r_s^2 \rangle$ at the level of $0.12 fm^2$. The measurement discussed in this proposal would improve the sensitivity to the strange charge radius by a further factor of three.

The approved G0 experiment in Hall C will make measurements off the proton over a range of Q^2 values at forward and backward angles. The most forward measurement will be at $\langle Q^2 \rangle \sim 0.16$ (GeV/c)^2, to be compared with 0.11 (GeV/c)^2 in this proposal. The statistical error to be achieved in both measurements is roughly the same. We note that the background environments offered by the G0 spectrometer and the Hall A HRS spectrometers are very different. Further, the G0 measurement will count individual events and reject background using time of flight information. This is in sharp contrast to the integration technique to be used in the proposal under discussion. In our opinion, the measurement of the parity violating asymmetry at such forward angles and at high luminosity is challenging and important enough to warrant two independent measurements at roughly the same level of accuracy.

Finally, we note that our collaboration is investigating the possibility of a follow up experiment using a ^{4}He target at roughly the same kinematics. The two measurements (^{1}H and ^{4}He) provide two different linear combinations of μ_s and ρ_s. The combined analysis would provide a constraint on $\langle r_s^2 \rangle$ to $\pm 0.022 fm^2$. Further, the two experiments would provide an independent

constraint on μ_s to $\pm 0.21 \mu_N$.

VIII CONCLUSION

We have described a new proposal to measure the parity violating asymmetry in forward angle elastic electron-proton scattering in order to signicantly constrain or measure the nucleon strangeness radius. The recent success of the HAPPEX experiment has demonstrated that systematic errors can be controlled at the required level with a high polarization strained GaAs photocathode. The experiment has further demonstrated that the HRS spectrometers in Hall A are ideally suited for a high counting rate parity violating experiment using the flux integration technique. This ensures that the measurement discussed in this proposal is feasible with little additional hardware.

REFERENCES

1. D.B. Kaplan and A. Manohar, Nucl. Phys. B **310**, 527 (1988)
2. R.D. McKeown, Phys. Lett. B **219**, 140 (1989), D.H. Beck, Phys. Rev. D **39**, 3248 (1989).
3. B. Mueller *et.al.*, Phys. Rev. Lett. **78**, 3824 (1997).
4. HAPPEX collaboration, Phys. Rev. Lett. **82**, 1096 (1999)
5. M.J. Musolf, T.W. Donnelly, J. Dubach, S.J. Pollock, S. Kowalski and E.J. Beise, Phys. Rep. **239**, 1-178 (1994)
6. C.Y. Prescott *et.al.*, Phys. Lett. B **84**, 524 (1979).
7. M.J. Ramsay-Musolf, hep-ph 9712317.
8. S. Galster *et. al.*, Nucl. Phys. **B32**, 221 (1971)
9. R.L. Jaffe, Phys. Lett. B **229**, 275 (1989)
10. H.W. Hammer, Ulf-G. Meissner and D. Drechsel, Phys. Lett. B **367**, 323 (1996)
11. Ulf-G. Meissner *et. al.*, hep-ph/9701296 (1997).
12. H.-W. Hammer and M.J. Ramsey-Musolf, hep-ph/9903367 (1999)
13. H. Weigel, A. Abada, R. Alkofer and H. Reinhardt, Phys. Lett. B **353**, 20 (1995)
14. N.W. Park, J. Schechter and H. Weigel, Phys. Rev. D **43**, 869 (1991)
15. N.W. Park and H. Weigel, Orsay Report IPNO/TH 91-57 (1991)
16. S.J. Dong, K.F. Liu and A.G. Williams, hep-ph 9712483, (1997).
17. P. Geiger and N. Isgur, hep-ph 9610445, (1996).
18. High Resolution 1p shell Hypernuclear Spectroscopy, Jlab proposal 94-107, S. Frullani, F. Garibaldi, P. Markowitz and T. Saito spokespersons.
19. A proposal for Two Septum Magnets for Forward Angle Physics in Hall A at TJNAF, Submitted to the TJNAF Technical Advisory Committee, Hypernuclear collaboration, (1996).
20. P. Gorodetzky *et. al.*, Nucl. Instr. Meth. A **361**, (1995), 161
    G. Anzivino *et. al.*, Nucl. Instr. Meth. A **357**, (1995), 369.
21. R. Michaels, Empirical Study of Background for HAPPEX in elastic Electron-Proton Scattering, private communication.
22. J.W Lightbody and J.S O'Connell, Computer in Physics may/june 1988
23. L. Koester, W. Nistler and W. Washkowski, Phys. Rev. Lett.**36**, (1976),1021
24. S. Platchkov *et. al.*, Nucl. Phys. **A510**, (1990), 740-758
25. C. Caso *et. al.*, The European Physical Journal **C3**, (1998), 1